

A Better Loss for Visual-Textual Grounding

Davide Rigoni,^{1, 2} Luciano Serafini,² Alessandro Sperduti¹

¹ University of Padua, Padua, Italy

² Fondazione Bruno Kessler, Povo, Italy

davide.rigoni.2@phd.unipd.it, serafini@fbk.eu, alessandro.sperduti@unipd.it

Abstract

Given a textual phrase and an image, the visual grounding problem is defined as the task of locating the content of the image referenced by the sentence. It is a challenging task that has several real-world applications in human-computer interaction, image-text reference resolution, and video-text reference resolution. In the last years, several works have addressed this problem with heavy and complex models that try to capture visual-textual dependencies better than before. These models are typically constituted by two main components that focus on how to learn useful multi-modal features for grounding and how to improve the predicted bounding box of the visual mention, respectively. Finding the right learning balance between these two sub-tasks is not easy, and the current models are not necessarily optimal with respect to this issue. In this work, we propose a model that, although using a simple multi-modal feature fusion component, is able to achieve a higher accuracy than state-of-the-art models thanks to the adoption of a more effective loss function, based on the classes probabilities, that reaches, in the considered datasets, a better learning balance between the two sub-tasks mentioned above.

1 Introduction

In the last years, the scientific community has devoted much effort in developing deep learning models for computer vision and natural language processing, thanks to the increasing computational resources and the availability of new data. While deep learning models for computer vision aim to interpret and understand the visual world made by images and videos, deep learning models for natural language processing aim to interpret and understand the human natural language. In the last decade, these two research areas have made outstanding advancements that have lead to the formulation of more complex problems in which both vision and textual information are required, such as visual-question answering (Antol et al. 2015; Shih, Singh, and Hoiem 2016; Zhou et al. 2015), image retrieval (Mao et al. 2014; Klein et al. 2014; Frome et al. 2013; Kiros, Salakhutdinov, and Zemel 2014), and visual grounding (Rohrbach et al. 2016; Chen, Gao, and Nevatia 2018; Zhang, Niu, and Chang 2018; Gupta et al. 2020). Among these, of particular interest is the visual grounding problem, defined as the task of locating the content of the image referenced by a given sentence, a building block for many other real-world applications and more

complex tasks. It is a challenging task, which requires the semantic understanding of the image content and its textual description, requiring the ability to predict the parts of the image content referred by a specific descriptive sentence. It can be formulated as an object detection task followed by a classification task in which, given an input image and sentence, the goal is to return only the detected object(s) in the image that represent the best semantic match with the sentence. In the initial phase of research on this problem, many works have followed this formulation, developing the so called two-stage approach models (Rohrbach et al. 2016; Yu et al. 2018), while more recent works have chosen to address the problem by a one-stage approach model, in which the object detection and the classification problem are solved jointly (Yang et al. 2019; Sadhu, Chen, and Nevatia 2019).

In the two-stage approach, the visual grounding model receives in input a set of proposal bounding boxes previously extracted by an object proposals extractor, such as Edge Boxes (Zitnick and Dollár 2014) and Selective Search (Uijlings et al. 2013), or by an object detector, such as Faster R-CNN (Ren et al. 2015), Single Shot multibox Detector (SSD) (Liu et al. 2016), or YOLO (Redmon et al. 2016; Redmon and Farhadi 2018). These proposals, jointly with the given input textual sentence describing the content of the image, constitute the visual grounding model input. Usually, the model embeds the sentence in an embedding representation that tries to capture its semantic content. Then, the model predicts, for each proposal bounding box, a score that represents how much the content of the bounding box is likely to be referred by the sentence. Often, the two-stage approach models predict new coordinates for the best predicted proposal, in order to adjust the coordinates to better fit the visual content according to the sentence semantic information.

In the one-stage approach, the visual grounding model receives in input only an image and a textual sentence. Then the model learns how to extract and fuse all the visual and textual information in order to predict the best bounding box in output, according to the input sentence. Even if this seems to be the best approach in order to reach the best results, due to the small number of assumptions made by the model, it raises some major issues: (*i*) not all the visual grounding datasets are suitable for training an object detector, due to lack of images and/or because they are not densely anno-

tated; (ii) the model requires an high number of parameters, and because of that (iii) the training requires significant computing resources.

In the literature, there are many works adopting increasingly improved object proposals, and increasingly complex architectures than before in order to capture the visual and textual information. These models are typically constituted by two main components that focus on how to learn useful multi-modal features for grounding, and how to improve the predicted bounding box of the visual mention, respectively. Finding the right learning balance between these two sub-tasks is not easy, and the current models are not necessarily optimal with respect to this issue. In this work, we propose a model that, although using a simple multi-modal feature fusion component, is able to reach a higher accuracy than state-of-the-art models thanks to the adoption of a more effective loss function that reaches a better learning balance between the two sub-tasks mentioned above. Our main contributions can be summarized as:

- we present a new grounding loss for visual proposals which considers also the object proposals semantic information, differently from the works in the literature which just consider their shapes and spatial positions in the image;
- we are the first to adopt the Complete Intersection over Union (Zheng et al. 2020b) loss for the visual grounding task;
- we introduce a new regression loss on the proposal bounding boxes coordinates which is applied to a subset of all the proposals, selected by considering the object proposals semantic information. This loss differs from the one used by the approaches in the literature, which only considers the proposal with the largest overlap with the ground truth.

This paper is structured as follows: Section 2 presents the state of the art approaches; Section 3 introduces notation and background; Section 4 presents our model architecture and losses; Section 5 presents our results; Section 6 reports the ablation study on the components of the losses, and Section 7 concludes this work.

2 Related Works

In this section, we report the most related works developed within three related areas, i.e. Referring Expression Grounding, Visual-Textual-Knowledge Entity Linking (VTKEL), and Image Retrieval.

Referring Expression Grounding It is also known as phrase localization or visual grounding. It aims to localize the corresponding objects described by a human natural language phrase in an image. It is common to extract visual and language features independently and fuse them before the prediction. Some works apply a multi layer perceptron (MLP) (Chen, Kovvuri, and Nevatia 2017; Chen, Gao, and Nevatia 2018), cosine similarity (Engilberge et al. 2018) and element-wise multiplication. Other works applies more complex strategies such as Canonical Correlation Analysis

(CCA) (Plummer et al. 2017a,b), Multimodal Compact Bilinear (MCB) (Fukui et al. 2016), graph structures (Bajaj, Wang, and Sigal 2019) and attention methods (Nguyen and Okatani 2018).

Instead of focusing on the fusion component, (Yu et al. 2018) proposes a visual grounding model with diverse and discriminative proposals that can achieve good performance without using a complex multi-modal fusion operator. The approach presented in (Akbari et al. 2019) predicts the image content location referred by the input phrase using an heatmap, applying a multi-level multi-modal attention mechanism, instead of relying on the standard bounding box. Some works focus on the weakly supervised referring expression grounding setting, in which it is available only the information about the image contents and there is no mapping among the input textual sentences and these visual locations. Given a set of bounding boxes proposals and a textual sentence in input, (Rohrbach et al. 2016) introduces a model which learns to ground by reconstructing the given textual sentence adopting a soft attention mechanism. This approach is extended in (Chen, Gao, and Nevatia 2018) by the introduction of a novel Knowledge Aided Consistency Network (KAC Net) which is optimized by reconstructing the input query and proposal’s information. A different approach is developed in (Xiao, Sigal, and Jae Lee 2017), where an end-to-end model learns to localize arbitrary linguistic phrases in the form of spatial attention masks, using two types of carefully designed loss functions. A Variational Context model, based on the variational Bayesian method, is adopted by (Zhang, Niu, and Chang 2018) to exploit the reciprocal relation between the referent and context. The Multi-scale Anchored Transformer Network (MATN) (Zhao et al. 2018) hinges on the concept of anchors, i.e. it uses region proposals as localization anchors, learning a multi-scale correspondence network to continuously search for sentences referring to the anchors. The work presented in (Gupta et al. 2020) shows that textual sentence grounding can be learned by optimizing word-region attention to maximize a lower bound on mutual information between images and caption words. (Liu et al. 2019) uses a cross-modal attention-guided erasing approach, where it discards the most dominant information from either textual or visual domains to generate difficult training samples online in order to drive the model to discover complementary textual-visual correspondences. (Deng et al. 2018) provides an accumulated attention (A-ATT) mechanism to ground the natural language query into the image using a query attention, an image attention and an objects attention.

Visual-Textual-Knowledge Entity Linking The new defined VTKEL task (Dost et al. 2020c,a,b) introduces a more complex task than the referring expression task, in which an artificial agent needs to jointly recognize the entities shown in the image and mentioned in the text, and to link them to its prior background knowledge. The solution to the VTKEL problem could lead to major scientific advancement towards a better understanding of semantic information contained in the image and textual sentence, respectively. In fact, the knowledge graph allows to introduce semantic reasoning on

the information contained in both the image and the textual sentence, which could lead to innovative solutions for the weakly supervised referring expression problem and for the partially annotated dataset problem.

Image Retrieval The standard text-base image retrieval systems, given a textual sentence in input, from a set of images select the one that best matches the textual input. In particular, the best images are returned according to some metric learned through a recurrent neural network (Mao et al. 2014), correlation analysis (Klein et al. 2014) and other methods (Frome et al. 2013; Kiros, Salakhutdinov, and Zemel 2014).

3 Background

In this section, we summarize the background notions needed to introduce our work.

3.1 Notation

In order to explain our work, we use the following notation: lower case symbols for scalars and indexes, e.g. n ; italics upper case symbols for sets, e.g. A ; upper case symbols for textual sentences, e.g. S ; bold lower case symbols for vectors, e.g. \mathbf{a} ; bold upper case symbols for matrices and tensors, e.g. \mathbf{A} ; the position within a tensor or vector is indicated with numeric subscripts, e.g. \mathbf{A}_{ij} with $i, j \in \mathbb{N}^+$; calligraphic symbols for domains, e.g. \mathcal{Q} .

3.2 Problem Definition

Visual grounding is the general task of locating the components of a structured description in an image. In order to solve this task, first, it is necessary to recognize all the objects in the image and the components in the text, while after, the model needs to find the correct alignment among the nouns and the objects. Each detected object in the image is usually represented by a rectangle called bounding box, while each noun phrase detected in the text is usually called query. The bounding box is determined by its position in the image and by its dimension, while the query is determined by the position of the first character and the position of the last character in the input text.

Formally, given in input an image \mathbf{I} and a sentence S describing some of the objects represented in \mathbf{I} , the task consists in learning a map γ from the set Q of noun phrases contained in S to a set of bounding boxes B defined on \mathbf{I} , i.e. $\gamma : \mathcal{I} \times \mathcal{S} \rightarrow 2^{Q \times \mathcal{B}}$, where \mathcal{I} is the domain of images, \mathcal{S} is the domain of sentences, Q is the noun phrases domain, \mathcal{B} is the domain of bounding boxes which can be defined on \mathcal{I} , and $2^{Q \times \mathcal{B}}$ is the power set of the Cartesian product between Q and \mathcal{B} . So, given an image \mathbf{I} containing e objects identified via the set of bounding boxes $B_{\mathbf{I}} = \{\mathbf{b}_i\}_{i=1}^e$, where $\mathbf{b}_i \in \mathbb{R}^4$ is the vector of coordinates identifying a bounding box in \mathbf{I} , and a sentence S containing m noun phrases gathered in the set $Q_S = \{\mathbf{q}_j\}_{j=1}^m$, where $\mathbf{q}_j \in \mathbb{N}^2$ is a vector containing as coordinates the initial and final character positions in the sentence S , $\gamma(\mathbf{I}, S)$ returns a set of couples $\{(\mathbf{q}, \mathbf{b}) | \mathbf{q} \in Q_S, \mathbf{b} \in B_{\mathbf{I}}\}$ where each couple (\mathbf{q}, \mathbf{b}) associates the noun phrase \mathbf{q} to the bounding box \mathbf{b} . Please, notice that the same noun phrase can be

associated to several different bounding boxes, as well as the same bounding box can be associated to many different noun phrases. Following the current literature, in this paper we assume that each noun phrase is associated to one and only one bounding box. Bounding boxes, however, can identify more objects, e.g. several persons in the case the noun phrase is “people”. A training set of n examples is defined as $D = \{(\mathbf{I}_i, S_i, \{(\mathbf{q}^{gt}, \mathbf{b}^{gt})\}_i\}_{i=1}^n$, where $\{(\mathbf{q}^{gt}, \mathbf{b}^{gt})\}_i$ is the set of ground truth associations for example i , i.e. $\gamma(\mathbf{I}_i, S_i) = \{(\mathbf{q}^{gt}, \mathbf{b}^{gt})\}_i$.

3.3 Intersection over Union (IoU)

Given a pair of bounding box coordinates $(\mathbf{b}_i, \mathbf{b}_j)$, the *Intersection over Union* (IoU), also known as Jaccard index, is an evaluation metric used mainly in object detection tasks, which aims to evaluate how much the two bounding box refer to the same content in the image. Specifically, it is defined as:

$$IoU(\mathbf{b}_i, \mathbf{b}_j) = \frac{|\mathbf{b}_i \cap \mathbf{b}_j|}{|\mathbf{b}_i \cup \mathbf{b}_j|}, \quad (1)$$

where $|\mathbf{b}_i \cap \mathbf{b}_j|$ is the area of the box obtained by the intersection of boxes \mathbf{b}_i and \mathbf{b}_j , while $|\mathbf{b}_i \cup \mathbf{b}_j|$ is the area of the box obtained by the union of boxes \mathbf{b}_i and \mathbf{b}_j . It is invariant to the bounding boxes sizes, and it returns values that are strictly contained in the interval $[0, 1] \subset \mathbb{R}$, where 1 means that the two bounding boxes refer to the same image area, while a score of 0 means that the two bounding boxes do not overlap at all. The fact that two bounding boxes that do not overlap have IoU score equal to 0, is the major issue of this metric: the zero value does not represent how much the two bounding boxes are far from each other. For this reason, in its standard definition, the intersection over union is mainly used as an evaluation metric rather than as a component of a loss function for learning.

3.4 Complete Intersection over Union (CIoU)

In order to solve the issue of IoU when considering it as a loss function, several alternative formulations were suggested in the literature, e.g. (Rezatofighi et al. 2019) proposed the *Generalized IoU* (GIoU) loss, (Zheng et al. 2020a) proposed the *Distance IoU* (DIoU) loss, while only recently (Zheng et al. 2020b) proposed the *Complete IoU* (CIoU) loss, which has shown promising results and faster convergence than GIoU and DIoU. It is defined as:

$$\mathcal{L}_{CIoU}(\mathbf{b}_i, \mathbf{b}_j) = S(\mathbf{b}_i, \mathbf{b}_j) + D(\mathbf{b}_i, \mathbf{b}_j) + V(\mathbf{b}_i, \mathbf{b}_j) \quad (2)$$

$$S(\mathbf{b}_i, \mathbf{b}_j) = 1 - IoU(\mathbf{b}_i, \mathbf{b}_j); \quad (3)$$

$$D(\mathbf{b}_i, \mathbf{b}_j) = \frac{\rho(\mathbf{p}_i, \mathbf{p}_j)^2}{c^2}; \quad (4)$$

$$V(\mathbf{b}_i, \mathbf{b}_j) = \alpha \frac{4}{\pi^2} \left(\arctan \frac{wt_j}{ht_j} - \arctan \frac{wt_i}{ht_i} \right) \quad (5)$$

where \mathbf{b}_i and \mathbf{b}_j are two bounding boxes, \mathbf{p}_i and \mathbf{p}_j are their central points, $IoU(\mathbf{b}_i, \mathbf{b}_j)$ is the standard IoU, ρ is the euclidean distance between the given points, c is the diagonal length of the *convex hull* of the two bounding boxes, α is a trade-off parameter, wt_i and ht_i are the width and

the height of the bounding box \mathbf{b}_i , respectively. Differently from the standard IoU, the Complete IoU is formulated to gives meaningful values, leveraging the bounding boxes geometric shapes, even when two bounding boxes are not overlapped.

4 Our Proposal

In this section, we first describe the structure of our model, and then we describe the training procedure, which exploits the original part of our proposal, e.g. a loss function composed of novel sub-losses.

4.1 Model

Our model, outlined in Figure 1, follows a typical basic architecture for visual-textual grounding tasks. It is based on a two-stage approach in which, initially, a pre-trained object detector is used to extract, from a given image \mathbf{I} , a set of k bounding box proposals $\mathcal{P}_I = \{\mathbf{p}_i\}_{i=1}^k$, where $\mathbf{p}_i \in \mathbb{R}^4$, jointly with features $H^v = \{\mathbf{h}_i^v\}_{i=1}^k$, where $\mathbf{h}_i^v \in \mathbb{R}^v$. The features represent the internal object detector activation values before the classification layers and regression layer for bounding boxes. Moreover, our model extracts the spatial features $H^s = \{\mathbf{h}_i^s\}_{i=1}^k$, where $\mathbf{h}_i^s \in \mathbb{R}^s$ from all the bounding boxes proposals, where the spatial features for the proposal \mathbf{p}_i are defined as:

$$\mathbf{h}_i^s = \left[\frac{x1}{wt}, \frac{y1}{ht}, \frac{x2}{wt}, \frac{y2}{ht}, \frac{(x2 - x1) \times (y2 - y1)}{wt \times ht} \right], \quad (6)$$

where $(x1, y1)$ refers to the top-left bounding box corner, $(x2, y2)$ refers to the bottom-right bounding box corner, wt and ht are the width and height of the image, respectively. We also assume that the object detector returns, for each \mathbf{p}_i , a probability distribution $Pr_{Cls}(\mathbf{p}_i)$ over a set $Clss$ of predefined classes, i.e. the probability for each class $\xi \in Clss$ that the content of the bounding box \mathbf{p}_i belongs to ξ . This information is typically returned by most of the object detectors, and it will be used to define our novel loss function.

Regarding the textual features extraction, given a noun phrase \mathbf{q}_j , initially all its words $W^{\mathbf{q}_j} = \{w_i^{\mathbf{q}_j}\}_{i=1}^l$ are embedded in a set of vectors $E^{\mathbf{q}_j} = \{e_i^{\mathbf{q}_j}\}_{i=1}^l$ where $e_i^{\mathbf{q}_j} \in \mathbb{R}^w$, where w is the size of the embedding. Then, our model applies a LSTM (Hochreiter and Schmidhuber 1997) neural network to generate from the sequence of word embeddings only one new embedding \mathbf{h}_j^* for each phrase \mathbf{q}_j . This textual features extraction is defined as:

$$\mathbf{h}_j^* = L1(LSTM(E^{\mathbf{q}_j})), \quad (7)$$

where $\mathbf{h}_j^* \in \mathbb{R}^t$ is the LSTM output of the last word in the noun phrase \mathbf{q}_j , and $L1$ is the L1 normalization function.

Once vector \mathbf{h}_j^* has been generated from the noun phrase \mathbf{q}_j , the model performs a multi-modal feature fusion operation in order to combine the information contained in \mathbf{h}_j^* with each of the proposal bounding boxes \mathbf{h}_i^v . For this operation, we have decided to use a simple function that merges the multi-modal features together rather than relying on a more complex operator, such as bilinear-pooling or deep neural network architectures. We leave the use of a more

complex fusion operator, that will lead to further improvements, for future work. The multi-modal fusion component we adopted returns the set of new vectorial representations $H^{\parallel} = \{\mathbf{h}_{jz}^{\parallel}\}_{j \in [1, \dots, m], z \in [1, \dots, k]}$, where vectors $\mathbf{h}_{jz}^{\parallel}$ are defined as:

$$\mathbf{h}_{jz}^{\parallel} = LR \left(\mathbf{W}^{\parallel} (\mathbf{h}_j^* \parallel \mathbf{h}_z^s \parallel L1(\mathbf{h}_z^v)) + \mathbf{b}^{\parallel} \right), \quad (8)$$

where \parallel indicates the concatenation operator, $\mathbf{h}_{jz}^{\parallel} \in \mathbb{R}^c$, LR indicates the leaky-relu activation function, $\mathbf{W}^{\parallel} \in \mathbb{R}^{c \times (t+s+v)}$ is a matrix of weights, and $\mathbf{b}^{\parallel} \in \mathbb{R}^c$ is a bias vector.

Finally, the model predicts the probability P_{jz} that a given noun phrase \mathbf{q}_j is referred to a proposal bounding box \mathbf{p}_z as:

$$P_{jz} = \frac{\exp(\mathbf{W}^g \times \mathbf{h}_{jz}^{\parallel} + b^g)}{\sum_{i=1}^k \exp(\mathbf{W}^g \times \mathbf{h}_{ji}^{\parallel} + b^g)}, \quad (9)$$

where $\mathbf{W}^g \in \mathbb{R}^{1 \times c}$ and $b^g \in \mathbb{R}$ are weights.

Indeed, the representations $\mathbf{h}_{jz}^{\parallel}$ of the proposals bounding box features conditioned with the textual features can also be used to refine the proposal bounding box coordinates, that are generated by the object detector independently by the textual features. Specifically, our model does not predicts new bounding box coordinates, but offsets for the coordinates defined as

$$\mathbf{o}_{jz} = \mathbf{W}^{\mathcal{B}} \times \mathbf{h}_{jz}^{\parallel} + \mathbf{b}^{\mathcal{B}}, \quad (10)$$

where $\mathbf{W}^{\mathcal{B}} \in \mathbb{R}^{4 \times c}$ and $\mathbf{b}^{\mathcal{B}} \in \mathbb{R}^4$ are a matrix of weights and a bias vector, respectively. The final predicted bounding boxes coordinates are then obtained as the sum of the proposal bounding boxes coordinates with the predicted offsets.

4.2 Training

In this section, we present the main novel contribution of the paper, i.e. a loss function composed of novel terms. For the sake of presentation, we define in the following the loss terms referred to a single example. The total loss is then obtained by summing up the contributions of all examples in the training set.

Given a training example $(\mathbf{I}, \mathbf{S}, \{(\mathbf{q}_j^{gt}, \mathbf{b}_j^{gt})\}_{j=1}^m)$, where m is the number of noun phrases, and the bounding box proposals set \mathcal{P}_I , we define the loss function \mathcal{L} (for a single example) as:

$$\mathcal{L} = \mathcal{L}_g(\mathbf{P}, \mathcal{P}_I, \{\mathbf{b}_j^{gt}\}) + \lambda \mathcal{L}_c(\mathcal{P}_I, \{\mathbf{b}_j^{gt}\}), \quad (11)$$

where \mathcal{L}_g is the loss used to “shape” the grounding distribution of bounding box proposals for each specific query in input, i.e. the probability that a given proposal is associated to a given query, \mathcal{L}_c is the loss related to the refinement of the bounding boxes coordinates, and λ is a trade-off parameter.

Differently from most of the previous works that use the *cross-entropy* (*CE*) loss or the standard *Kullback–Leibler* (*KL*) divergence loss for grounding, our model implements a *KL* divergence loss in which the ground truth probability is built also considering $Pr_{Cls}(\mathbf{p}_i)$ with

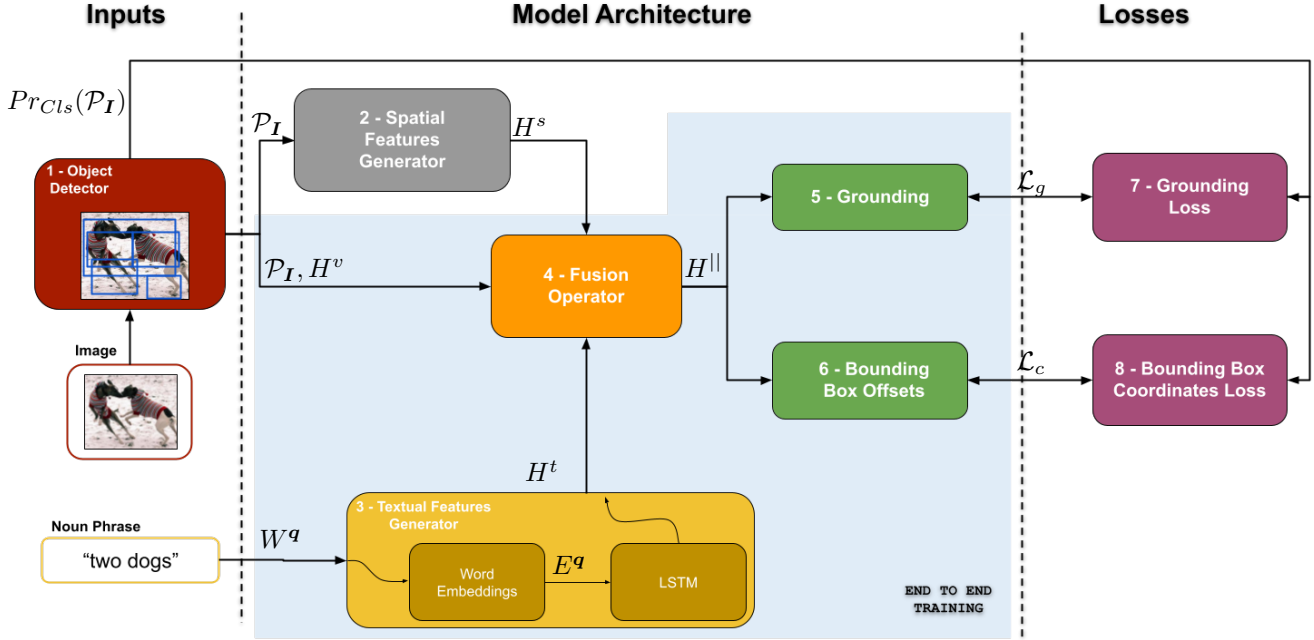


Figure 1: Our two-stage model architecture overview. (1) Initially, the image is processed by a pre-trained *Faster R-CNN* object detector in order to extract all the proposals bounding boxes from which (2) the spatial features are generated. Then, the model (3) generates the textual features from the input noun phrase using the *Textual Features Generator* module, by first retrieving each word embedding and then using an LSTM network. Finally, the model (4) fuses together all the visual, spatial, and textual features by the *Fusion Operator*, obtaining new features that are then used in the (5) *Grounding* and (6) *Bounding Box Offsets* modules, respectively. Our defined losses \mathcal{L}_g (7) and \mathcal{L}_c (8) are used in order to train the network end-to-end on the components included in the light blue background.

$\mathbf{p}_i \in \mathcal{P}_I$, i.e. the semantic information associated to bounding box proposals. Specifically, we define the entries ($j \in [1, \dots, m]$, $z \in [1, \dots, k]$) of matrix \mathbf{U} as:

$$U_{jz} = IoU(\mathbf{p}_z, \mathbf{b}_j^{gt}), \quad (12)$$

the best proposal bounding box as \mathbf{p}_{j*} where:

$$j* = \operatorname{argmax}_{z \in [1, \dots, k]} U_{jz}, \quad (13)$$

and the entries ($j \in [1, \dots, m]$, $z \in [1, \dots, k]$) of matrix \mathbf{C} containing the cosine similarity scores among the predicted class probabilities of the bounding box proposals as:

$$C_{jz} = Sim(Pr_{C_{cls}}(\mathbf{p}_{j*}), Pr_{C_{cls}}(\mathbf{p}_z)), \quad (14)$$

where Sim is the cosine similarity function. Given these definitions, we can define the entries of the ground truth probability \mathbf{P}^{gt} as:

$$\mathbf{P}_{jz}^{gt} = \frac{\mathbf{U}_{jz}^*}{\sum_{i=1}^k \mathbf{U}_{ji}^*}, \quad (15)$$

where

$$\mathbf{U}_{jz}^* = \begin{cases} \mathbf{U}_{jz} \times \mathbf{C}_{jz}, & \text{if } \mathbf{U}_{jz} \geq \eta \\ 0, & \text{otherwise} \end{cases}, \quad (16)$$

and η is a predefined threshold, i.e. an hyper-parameter.

On the basis of the above definitions, we define the grounding loss as:

$$\mathcal{L}_g(\mathbf{P}, \mathcal{P}_I, \{\mathbf{b}_j^{gt}\}) = \frac{1}{m} \sum_{j=1}^m KL_{div}(\mathbf{P}_j || \mathbf{P}_j^{gt}), \quad (17)$$

$$= \frac{1}{m} \sum_{j=1}^m \sum_{z=1}^k \mathbf{P}_{jz} \log \left(\frac{\mathbf{P}_{jz}}{\mathbf{P}_{jz}^{gt}} \right), \quad (18)$$

where \mathbf{P}_j (\mathbf{P}_j^{gt}) is the j -th row of \mathbf{P} (\mathbf{P}^{gt}), m is the number of noun phrases, k is the number of proposal bounding boxes, and \mathbf{P}_{jz} is the model predicted probability that the noun phrase $q_j \in Q$ refers to the image content localized by $\mathbf{p}_z \in \mathcal{P}_I$.

Indeed, the grounding loss captures both the bounding box spatial information and the semantic information determined by the bounding box classes. Whenever a bounding box is located near the ground truth bounding box and its class probability distribution is similar to the one of the best proposal \mathbf{p}_{j*} , then the loss favours the prediction of the bounding box, otherwise the loss penalizes the bounding boxes according to their different probability distribution and spatial location. Previous works exploiting the KL divergence aims to maximize the probability of a proposal bounding box just considering their spatial location.

Regarding the bounding boxes coordinates refinement, differently from previous works that use the *SmoothL1* loss,

our model adopts the *Complete IoU loss* (Zheng et al. 2020b). To the best of our knowledge, this is the first work adopting the *Complete IOU* loss in order to refine the final bounding boxes coordinates. Moreover, differently from all the works in the literature in which the coordinates refinement loss is calculated only on the best proposal \mathbf{p}_{j*} coordinates, our loss, given a query \mathbf{q}_j , penalizes the subset $\mathcal{S}_j \subseteq \mathcal{P}_I$ defined as:

$$\mathcal{S}_j = \{\mathbf{p}_z \mid \mathbf{p}_z \in \mathcal{P}_I \wedge \mathbf{U}_{jz}^* \geq 0\}. \quad (19)$$

Specifically, given a query $\mathbf{q}_j \in Q$, our loss \mathcal{L}_c is defined as:

$$\mathcal{L}_c(\mathcal{P}_I, \{\mathbf{b}_j^{gt}\}) = \frac{1}{m} \sum_{j=1}^m \sum_{z=1}^{|\mathcal{S}_j|} \mathcal{L}_{CIoU}(\mathbf{p}_z, \mathbf{b}_j^{gt}) \times \hat{\mathbf{U}}_{jz}, \quad (20)$$

$$\hat{\mathbf{U}}_{jz} = \frac{\mathbf{U}_{jz}^*}{\max_{z \in [1, k]} \mathbf{U}_{jz}^* + \epsilon}, \quad (21)$$

in which ϵ is a small value added to avoid division by 0, and $\max_{z \in [1, k]}$ is the maximum function applied along the indexes $z \in [1, k]$. Intuitively, for each bounding box proposal which overlaps with the ground truth (according to the parameter η), this loss refines the coordinates proportionally to the “semantic” of the bounding box. Note that adopting the normalized scores $\hat{\mathbf{U}}_{jz}$, the model does not penalized the loss on the best proposal bounding box $j*$.

We would like to highlight that our work is the first proposing the exploitation of the probabilities distributions over the object detector classes to address the supervised visual grounding task. However, in weakly-supervised visual-textual grounding (*not our task*) some works (e.g. (Wang and Specia 2019)) leverage the information of the bounding box class with the *highest* probability.

5 Experimental Assessment

We have compared our model results on two widely adopted datasets considering several competing approaches in the literature, including state-of-the-art models.

5.1 Datasets

For the experimental assessment, we have chosen the two most common datasets used in the literature, although other data sets are present in the literature (e.g. (Chen et al. 2020; Kazemzadeh et al. 2014a; Yu et al. 2016; Mao et al. 2016)). Follow their description.

Flickr30K The Flickr30K Entities (Plummer et al. 2017b; Young et al. 2014) dataset contains 32K images, 275K bounding boxes, 159K sentences, and 360K noun phrases. Each image is associated with five sentences with a variable number of noun phrases, and each noun phrase is associated with a set of bounding boxes ground truth coordinates. Following all works in the literature, if a noun phrase corresponds to multiple ground truth bounding boxes, we merged the boxes and used their union region as its ground-truth. On the contrary, if a noun phrase has no associated bounding box, we removed it from the dataset. We used the standard split for training, validation, and test set as defined in (Plummer et al. 2017b), consisting of 30K, 1K, and 1K images, respectively.

Referit The Referit (Kazemzadeh et al. 2014b) dataset contains 20K images, 99K bounding boxes, and 130K noun phrases. This dataset differs from Flickr30k since it does not contain sentences, which means that the noun phrases are mutually independent. For this reason, the state-of-the-art models that depend on a sentence linking all the noun phrases, since they use a feature fusion operator that assumes the presence of the input sentence containing all the noun phrases, cannot be applied to it. We used the same split as in (Plummer et al. 2017b) that consists of 9K images of training, 1K images of validation, and 10K images of test.

5.2 Evaluation Metric

Aligned with the works in the literature, we consider the standard *accuracy* metric. Given a noun phrase, it considers a bounding box prediction to be correct if and only if the intersection over union value between the predicted bounding box and the ground truth bounding box is at least 0.5.

5.3 Implementation Details

Our model extracts the words vocabulary using the SpaCy (Honnibal et al. 2020) framework for both datasets. Each word embedding is initialized using the GloVe (Pennington, Socher, and Manning 2014) pre-trained weights, which our model does not train, while the remaining weights are initialized according to Xavier (Glorot and Bengio 2010). To compare objectively the experimental results with state-of-the-art models, we have used the same object detector adopted in (Yu et al. 2018), which consists of a Faster R-CNN pre-trained object detector (Anderson et al. 2018) on the Visual Genome (Krishna et al. 2017) dataset that uses ResNet-101 as backbone model¹. The features associated to each bounding box are extracted from the ResNet-101’s layer *pool5_flat*. Following (Yu et al. 2018), our object detector returns for each bounding box proposal a probability distribution over 1600 classes. We could have applied other object detectors or bounding box proposals which would have lead to further improvements, however this research direction is not related to the aim of this paper. Our model adopts the normalized bounding boxes coordinates with the following representation:

$$\mathbf{b} = \left[\frac{x1 + x2}{2}, \frac{y1 + y2}{2}, bwt, bht \right], \quad (22)$$

where $(x1, y1)$ refers to the top-left bounding box corner, $(x2, y2)$ refers to the bottom-right bounding box corner, bwt and bht are the width and height of the bounding box, respectively. Regarding the parameter *alpha* in Eq. 5, we just used the value specified in (Zheng et al. 2020b) which is identified by a specific formula.

5.4 Model Selection

To evaluate our model on the test set of Flickr30k and Referit datasets, we have chosen the epoch in which the model achieved the best accuracy metric on the validation set. We have performed a grid search for the best

¹The ResNet-101 weights were pre-trained on COCO for initialization.

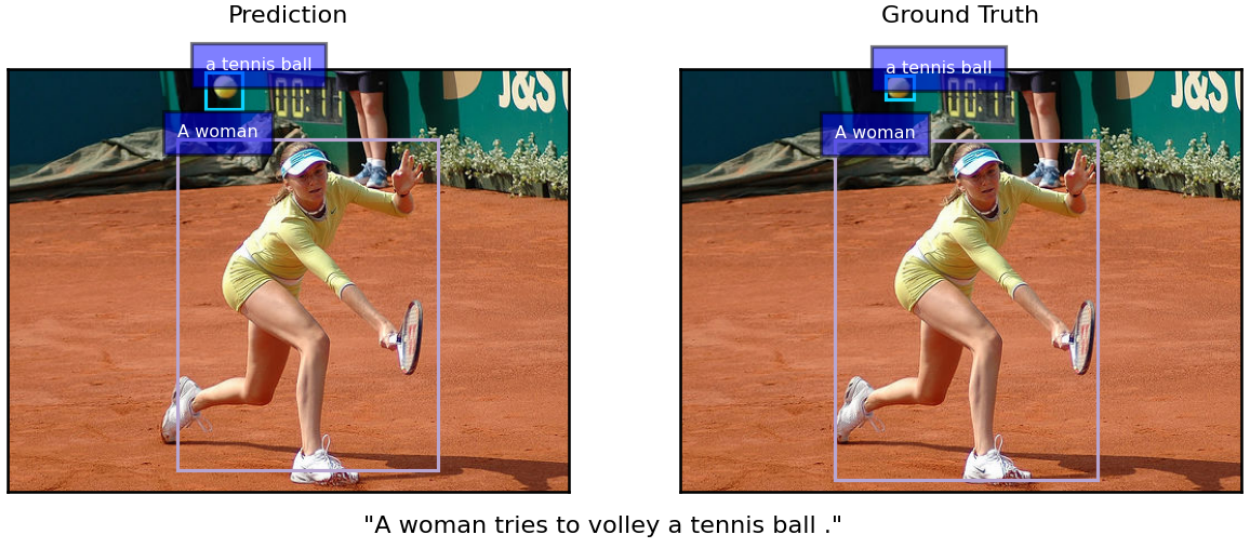


Figure 2: This picture reports a qualitative example of our model on the test image id: 23016347. The bounding boxes associated with each query are reported in the left picture, while the ground truth is reported in the right picture. The complete sentence in input is reported at the bottom of the figure. The prediction for the query “a tennis ball” is evaluated as wrong, even if the bounding box is very close to the ground truth.

hyper-parameters mainly for the Flickr30k dataset, ad exception of the losses hyper-parameters which can be seen in Section 6. For the Referit dataset, we have used the hyper-parameters values selected on the Flickr30k dataset. We have used the Adam optimizer with exponential learning rate scheduler set to 0.9, and the following values for the learning rate: $\{0.05, 0.03, 0.01, 0.005, 0.001\}$, $\eta : \{0.1, 0.3, 0.4, 0.45, 0.5, 0.55\}$, $c : \{2048, 2053, 2060\}$. Other hyper-parameters are fixed to single values. For the textual features: $w = 300$, $t = 500$, and the LSTM network uses only one hidden layer of dimension t . For the image features, we have extracted a fixed number $k = 100$ of proposals for each image, $v = 2048$ from the ResNet-101’s layer *pool5_flat*, and $s = 5$. In both datasets, we have found that the best model accuracy is achieved at epoch 9 of training with learning rate set to 0.001 and $c = 2053$. For Flickr30k we have set $\eta = 0.3$ and $\lambda = 1$, while for Referit we have set $\eta = 0.5$ and $\lambda = 1.4$.

5.5 Results

Table 1 reports the results obtained on the Flickr30k dataset by our approach and many other approaches presented in the literature, including the most recent state-of-the-art models reported at the bottom part of the table. Concerning the model CMGN developed in (Liu et al. 2020), for the sake of a fair comparison, we have reported the performance obtained using the same setting of our model. In fact, the complete version of the CMGN model achieves an accuracy of 76.74%, but exploiting query dependency information that we could exploit as well. The integration of this information in our model is left for future work. It can be noted that our approach significantly improves over competing approaches.

Model	Accuracy (%)
SCRC (Hu et al. 2016)	27.80
SMPL (Wang et al. 2016)	42.08
NonlinearSP (Wang, Li, and Lazebnik 2016)	43.89
GroundeR (Rohrbach et al. 2016)	47.81
MCB (Fukui et al. 2016)	48.69
RtP (Plummer et al. 2015)	50.89
Similarity Network (Wang et al. 2018)	51.05
IGOP (Yeh et al. 2017)	53.97
SPC+PPC (Plummer et al. 2017a)	55.49
SS+QRN (Chen, Kovvuri, and Nevatia 2017)	55.99
SeqGROUND (Dogan, Sigal, and Gross 2019)	61.60
CITE (Plummer et al. 2018)	61.89
QRC net (Chen, Kovvuri, and Nevatia 2017)	65.14
YOLO (Yang et al. 2019)	68.69
DDPN (Yu et al. 2018)	73.30
CMGN (Liu et al. 2020)*	73.46
SL-CCRF (Liu and Hockenmaier 2019)	74.69
Ours	75.55

Table 1: Results obtained on Flickr30k test set. Accuracy indicates in percentage the standard accuracy metric. All values are copied from the original articles. “*” indicates that the reported model accuracy is referring to the version of the model in their ablation study, since the complete model uses query dependency information that we do not exploit.

Table 2 reports the results obtained on the Referit dataset by our approach and the subset of the competing approaches reported in Table 1 that can be applied to this dataset, plus additional approaches that have been assessed on this dataset². Our model improves the accuracy value by 3.02%

²Some of them do not define an acronym, so we just use the

Model	Accuracy (%)
SCRC (Hu et al. 2016)	17.93
GroundeR (Rohrbach et al. 2016)	26.93
MCB (Fukui et al. 2016)	28.91
CITE (Plummer et al. 2018)	34.13
IGOP (Yeh et al. 2017)	34.70
(Wu, Xu, and Yang 2017)	36.18
QRC net (Chen, Kovvuri, and Nevatia 2017)	44.10
(Li et al. 2017)	44.20
(Yang et al. 2019)	59.30
DDPN (Yu et al. 2018)	63.00
Ours	66.02

Table 2: Results obtained on Referit test set. *Accuracy* indicates in percentage the standard accuracy metric. All values are reported from the original articles.

when compared to the state-of-the-art model (i.e., DDPN) for this dataset, representing a more significant gain than the one obtained on Flickr30k. In the Referit dataset, each sentence corresponds to a single query independent from the others. In contrast, in Flickr30k, a sentence could contain more queries that are semantically related among them. For this reason, models that apply complex multi-modal feature fusion components that aim to capture information among the queries extracted by the sentence in input sometimes do not consider the Referit dataset. Thus, the set of the model used as comparison in the Referit dataset is not the same as in Flickr30k and these reasons could explain the higher gain in accuracy obtained in Referit than Flickr30k.

We have also calculated the point game accuracy which is recently used for a few models addressing the weakly-supervised task. It considers a prediction to be correct if and only if the center of the predicted bounding box is contained in the ground truth bounding box. In particular, our model obtains 87.96% and 78.0% on Flickr30k and Referit, respectively. These values are far better than the ones reported in the literature for few models, and they suggest that a significant subset of predictions that are considered to be wrong according to the accuracy metric, still refer to bounding boxes that have a significant overlap with the ground truth.

5.6 Qualitative Results

Figure 2 shows a qualitative example predicted by our model. The example considers a Flickr30k test image with one of its five sentences. For each query extracted from the selected sentence reported at the bottom of the figure, on the left picture its predicted bounding box is reported. Similarly, on the right picture its ground truth is reported as well. In our model predictions, we have noticed that when the query refers to a small object in the image, most of the time our model predicts a very close bounding box, but not enough to have the IoU score over the 0.5 value. This is the case for the query “a tennis ball” in the figure.

6 Ablation Study

Our loss is composed by two main components and by two hyper-parameters. In this section, we report the contribution of each part of the loss using different hyper-parameters values. We have performed a set of experiments where the grounding component is alternatively the cross-entropy or the proposed semantic KL, and the regression component is alternatively the Smooth L1 or the proposed semantic CIoU. Moreover, different values for the hyper-parameters are considered. The obtained results (Table 3) show that the major contribution to the improvement is given by the *Complete IoU loss with semantic information*, which improves the model accuracy by $\sim 2.6\%$ and $\sim 3.9\%$ on Flickr30k and Referit datasets, respectively. Significant improvements are also obtained by using the semantic KL in place of cross-entropy. Moreover, results show that our approach is not much sensitive with respect to the hyper-parameters values, and, more importantly, the accuracy on the validation set indeed represents well the accuracy on the test set on both datasets.

7 Conclusion and Feature Work

This paper introduced a novel loss for Visual-Textual Grounding, jointly with a simple two-stage approach model. The novel loss combines a grounding loss and a bounding box coordinates refinement loss, both based on semantic information, i.e. a probability distribution over a set of pre-

reference to the paper.

Losses		Hyper-par.		Flickr30k (%)		Referit (%)	
Gr.	Reg.	λ	η	Val.	Test	Val.	Test
CE	SmoothL1	0.8	/	71.25	71.82	64.24	61.81
		1	/	71.08	71.61	64.19	61.29
	KL-Sem	0.8	0.4	72.22	72.72	64.38	61.78
		0.8	0.5	72.42	72.41	64.99	62.12
		1	0.4	72.54	72.88	65.04	62.47
		1	0.5	72.34	72.83	65.45	62.72
CE	CIoU-Sem	0.8	0.4	73.99	74.56	67.66	65.47
		0.8	0.5	73.60	74.24	67.41	65.07
		1	0.4	74.07	74.82	67.60	65.42
		1	0.5	73.90	74.24	67.24	65.15
KL-Sem	CIoU-Sem	0.6	0.5	75.17	75.38	68.23	66.31
		0.8	0.5	75.27	75.67	68.70	66.12
		1	0.5	75.41	75.53	68.72	66.52
		1.2	0.5	75.23	75.34	68.88	66.37
		1.4	0.5	75.13	75.36	68.97	66.02
		1	0.3	75.60	<u>75.55</u>	68.64	66.49
		1	0.4	75.40	75.64	68.56	66.54
		1	0.6	74.48	74.68	68.02	65.31

Table 3: Accuracy obtained on Flickr30k and Referit datasets as the losses functions and hyper-parameters values change. *CE* indicates the cross-entropy loss, *SmoothL1* indicates the Smooth L1 loss, *Kl-Sem* indicates our KL loss with the semantic information and *CIoU-Sem* indicate our Complete IoU loss with the semantic information. The baseline model does not use the η parameter.

defined classes, returned by the object detector. The experimental assessment showed that the proposed approach was able to reach a higher accuracy than state-of-the-art models, even without using a more complex multi-modal feature fusion component. Specifically, we have compared our results versus several models in the literature over two commonly used datasets, Flickr30k and Referit. With respect to the best state-of-the-art approaches, on the Flickr30k dataset, we obtained an improvement of 0.86%, while on the Referit dataset, our model improved the state-of-the-art performance by 3.02%.

Since this model uses a simple multi-modal feature fusion component, there is space for trivial improvements, including a more sophisticated multi-modal feature fusion component, such as bilinear-pooling and deeper architectures, as well as the exploitation of dependencies among the queries contained by the input sentence. Future work will also address more sophisticated object detectors, and the idea to include different forms of information, such as a scene graph and prior knowledge.

References

Akbari, H.; Karaman, S.; Bhargava, S.; Chen, B.; Vondrick, C.; and Chang, S.-F. 2019. Multi-level multimodal common semantic space for image-phrase grounding. In *Proceedings of the IEEE/CVF Conference on Computer Vision and Pattern Recognition*, 12476–12486.

Anderson, P.; He, X.; Buehler, C.; Teney, D.; Johnson, M.; Gould, S.; and Zhang, L. 2018. Bottom-Up and Top-Down Attention for Image Captioning and Visual Question Answering. In *CVPR*.

Antol, S.; Agrawal, A.; Lu, J.; Mitchell, M.; Batra, D.; Zitnick, C. L.; and Parikh, D. 2015. Vqa: Visual question answering. In *Proceedings of the IEEE international conference on computer vision*, 2425–2433.

Bajaj, M.; Wang, L.; and Sigal, L. 2019. G3raphground: Graph-based language grounding. In *Proceedings of the IEEE/CVF International Conference on Computer Vision*, 4281–4290.

Chen, K.; Gao, J.; and Nevatia, R. 2018. Knowledge aided consistency for weakly supervised phrase grounding. In *Proceedings of the IEEE Conference on Computer Vision and Pattern Recognition*, 4042–4050.

Chen, K.; Kovvuri, R.; and Nevatia, R. 2017. Query-guided regression network with context policy for phrase grounding. In *Proceedings of the IEEE International Conference on Computer Vision*, 824–832.

Chen, Z.; Wang, P.; Ma, L.; Wong, K.-Y. K.; and Wu, Q. 2020. Cops-Ref: A New Dataset and Task on Compositional Referring Expression Comprehension. In *Proceedings of the IEEE/CVF Conference on Computer Vision and Pattern Recognition (CVPR)*.

Deng, C.; Wu, Q.; Wu, Q.; Hu, F.; Lyu, F.; and Tan, M. 2018. Visual Grounding via Accumulated Attention. In *2018 IEEE Conference on Computer Vision and Pattern Recognition, CVPR 2018, Salt Lake City, UT, USA, June 18-22, 2018*, 7746–7755. IEEE Computer Society.

Dogan, P.; Sigal, L.; and Gross, M. 2019. Neural sequential phrase grounding (seqground). In *Proceedings of the IEEE/CVF Conference on Computer Vision and Pattern Recognition*, 4175–4184.

Dost, S.; Serafini, L.; Rospocher, M.; Ballan, L.; and Sperduti, A. 2020a. Jointly Linking Visual and Textual Entity Mentions with Background Knowledge. In *International Conference on Applications of Natural Language to Information Systems*, 264–276. Springer.

Dost, S.; Serafini, L.; Rospocher, M.; Ballan, L.; and Sperduti, A. 2020b. On Visual-Textual-Knowledge Entity Linking. In *2020 IEEE 14th International Conference on Semantic Computing (ICSC)*, 190–193. IEEE.

Dost, S.; Serafini, L.; Rospocher, M.; Ballan, L.; and Sperduti, A. 2020c. VTKEI: a resource for visual-textual-knowledge entity linking. In *Proceedings of the 35th Annual ACM Symposium on Applied Computing*, 2021–2028.

Engilberge, M.; Chevallier, L.; Pérez, P.; and Cord, M. 2018. Deep semantic-visual embedding with localization. In *RFIAP 2018-Congrès Reconnaissance des Formes, Image, Apprentissage et Perception*.

Frome, A.; Corrado, G. S.; Shlens, J.; Bengio, S.; Dean, J.; Ranzato, M.; and Mikolov, T. 2013. DeViSE: A Deep Visual-Semantic Embedding Model. In Burges, C. J. C.; Bottou, L.; Ghahramani, Z.; and Weinberger, K. Q., eds., *Advances in Neural Information Processing Systems 26: 27th Annual Conference on Neural Information Processing Systems 2013. Proceedings of a meeting held December 5-8, 2013, Lake Tahoe, Nevada, United States*, 2121–2129.

Fukui, A.; Park, D. H.; Yang, D.; Rohrbach, A.; Darrell, T.; and Rohrbach, M. 2016. Multimodal Compact Bilinear Pooling for Visual Question Answering and Visual Grounding. In Su, J.; Carreras, X.; and Duh, K., eds., *Proceedings of the 2016 Conference on Empirical Methods in Natural Language Processing, EMNLP 2016, Austin, Texas, USA, November 1-4, 2016*, 457–468. The Association for Computational Linguistics.

Glorot, X.; and Bengio, Y. 2010. Understanding the difficulty of training deep feedforward neural networks. In *Proceedings of the thirteenth international conference on artificial intelligence and statistics*, 249–256. JMLR Workshop and Conference Proceedings.

Gupta, T.; Vahdat, A.; Chechik, G.; Yang, X.; Kautz, J.; and Hoiem, D. 2020. Contrastive learning for weakly supervised phrase grounding. *arXiv preprint arXiv:2006.09920*.

Hochreiter, S.; and Schmidhuber, J. 1997. Long short-term memory. *Neural computation*, 9(8): 1735–1780.

Honnibal, M.; Montani, I.; Van Landeghem, S.; and Boyd, A. 2020. spaCy: Industrial-strength Natural Language Processing in Python.

Hu, R.; Xu, H.; Rohrbach, M.; Feng, J.; Saenko, K.; and Darrell, T. 2016. Natural language object retrieval. In *Proceedings of the IEEE Conference on Computer Vision and Pattern Recognition*, 4555–4564.

Kazemzadeh, S.; Ordonez, V.; Matten, M.; and Berg, T. 2014a. Referitgame: Referring to objects in photographs

of natural scenes. In *Proceedings of the 2014 conference on empirical methods in natural language processing (EMNLP)*, 787–798.

Kazemzadeh, S.; Ordonez, V.; Matten, M.; and Berg, T. L. 2014b. ReferIt Game: Referring to Objects in Photographs of Natural Scenes. In *EMNLP*.

Kiros, R.; Salakhutdinov, R.; and Zemel, R. S. 2014. Unifying visual-semantic embeddings with multimodal neural language models. *arXiv preprint arXiv:1411.2539*.

Klein, B.; Lev, G.; Sadeh, G.; and Wolf, L. 2014. Fisher vectors derived from hybrid gaussian-laplacian mixture models for image annotation. *arXiv preprint arXiv:1411.7399*.

Krishna, R.; Zhu, Y.; Groth, O.; Johnson, J.; Hata, K.; Kravitz, J.; Chen, S.; Kalantidis, Y.; Li, L.-J.; Shamma, D. A.; et al. 2017. Visual genome: Connecting language and vision using crowdsourced dense image annotations. *International journal of computer vision*, 123(1): 32–73.

Li, J.; Wei, Y.; Liang, X.; Zhao, F.; Li, J.; Xu, T.; and Feng, J. 2017. Deep Attribute-preserving Metric Learning for Natural Language Object Retrieval. In Liu, Q.; Lienhart, R.; Wang, H.; Chen, S. K.; Boll, S.; Chen, Y. P.; Friedland, G.; Li, J.; and Yan, S., eds., *Proceedings of the 2017 ACM on Multimedia Conference, MM 2017, Mountain View, CA, USA, October 23-27, 2017*, 181–189. ACM.

Liu, J.; and Hockenmaier, J. 2019. Phrase Grounding by Soft-Label Chain Conditional Random Field. In Inui, K.; Jiang, J.; Ng, V.; and Wan, X., eds., *Proceedings of the 2019 Conference on Empirical Methods in Natural Language Processing and the 9th International Joint Conference on Natural Language Processing, EMNLP-IJCNLP 2019, Hong Kong, China, November 3-7, 2019*, 5111–5121. Association for Computational Linguistics.

Liu, W.; Anguelov, D.; Erhan, D.; Szegedy, C.; Reed, S.; Fu, C.-Y.; and Berg, A. C. 2016. Ssd: Single shot multibox detector. In *European conference on computer vision*, 21–37. Springer.

Liu, X.; Wang, Z.; Shao, J.; Wang, X.; and Li, H. 2019. Improving referring expression grounding with cross-modal attention-guided erasing. In *Proceedings of the IEEE/CVF Conference on Computer Vision and Pattern Recognition*, 1950–1959.

Liu, Y.; Wan, B.; Zhu, X.; and He, X. 2020. Learning Cross-Modal Context Graph for Visual Grounding. In *The Thirty-Fourth AAAI Conference on Artificial Intelligence, AAAI 2020, The Thirty-Second Innovative Applications of Artificial Intelligence Conference, IAAI 2020, The Tenth AAAI Symposium on Educational Advances in Artificial Intelligence, EAAI 2020, New York, NY, USA, February 7-12, 2020*, 11645–11652. AAAI Press.

Mao, J.; Huang, J.; Toshev, A.; Camburu, O.; Yuille, A. L.; and Murphy, K. 2016. Generation and comprehension of unambiguous object descriptions. In *Proceedings of the IEEE conference on computer vision and pattern recognition*, 11–20.

Mao, J.; Xu, W.; Yang, Y.; Wang, J.; Huang, Z.; and Yuille, A. 2014. Deep captioning with multimodal recurrent neural networks (m-rnn). *arXiv preprint arXiv:1412.6632*.

Nguyen, D.-K.; and Okatani, T. 2018. Improved fusion of visual and language representations by dense symmetric co-attention for visual question answering. In *Proceedings of the IEEE Conference on Computer Vision and Pattern Recognition*, 6087–6096.

Pennington, J.; Socher, R.; and Manning, C. D. 2014. Glove: Global vectors for word representation. In *Proceedings of the 2014 conference on empirical methods in natural language processing (EMNLP)*, 1532–1543.

Plummer, B. A.; Kordas, P.; Kiapour, M. H.; Zheng, S.; Piramuthu, R.; and Lazebnik, S. 2018. Conditional image-text embedding networks. In *Proceedings of the European Conference on Computer Vision (ECCV)*, 249–264.

Plummer, B. A.; Mallya, A.; Cervantes, C. M.; Hockenmaier, J.; and Lazebnik, S. 2017a. Phrase Localization and Visual Relationship Detection with Comprehensive Image-Language Cues. In *IEEE International Conference on Computer Vision, ICCV 2017, Venice, Italy, October 22-29, 2017*, 1946–1955. IEEE Computer Society.

Plummer, B. A.; Wang, L.; Cervantes, C. M.; Caicedo, J. C.; Hockenmaier, J.; and Lazebnik, S. 2015. Flickr30k entities: Collecting region-to-phrase correspondences for richer image-to-sentence models. In *Proceedings of the IEEE international conference on computer vision*, 2641–2649.

Plummer, B. A.; Wang, L.; Cervantes, C. M.; Caicedo, J. C.; Hockenmaier, J.; and Lazebnik, S. 2017b. Flickr30K Entities: Collecting Region-to-Phrase Correspondences for Richer Image-to-Sentence Models. *IJCV*, 123(1): 74–93.

Redmon, J.; Divvala, S.; Girshick, R.; and Farhadi, A. 2016. You only look once: Unified, real-time object detection. In *Proceedings of the IEEE conference on computer vision and pattern recognition*, 779–788.

Redmon, J.; and Farhadi, A. 2018. Yolov3: An incremental improvement. *arXiv preprint arXiv:1804.02767*.

Ren, S.; He, K.; Girshick, R.; and Sun, J. 2015. Faster r-cnn: Towards real-time object detection with region proposal networks. *arXiv preprint arXiv:1506.01497*.

Rezatofighi, H.; Tsoi, N.; Gwak, J.; Sadeghian, A.; Reid, I.; and Savarese, S. 2019. Generalized intersection over union: A metric and a loss for bounding box regression. In *Proceedings of the IEEE/CVF Conference on Computer Vision and Pattern Recognition*, 658–666.

Rohrbach, A.; Rohrbach, M.; Hu, R.; Darrell, T.; and Schiele, B. 2016. Grounding of textual phrases in images by reconstruction. In *European Conference on Computer Vision*, 817–834. Springer.

Sadhu, A.; Chen, K.; and Nevatia, R. 2019. Zero-shot grounding of objects from natural language queries. In *Proceedings of the IEEE/CVF International Conference on Computer Vision*, 4694–4703.

Shih, K. J.; Singh, S.; and Hoiem, D. 2016. Where to look: Focus regions for visual question answering. In *Proceedings of the IEEE conference on computer vision and pattern recognition*, 4613–4621.

Uijlings, J. R.; Van De Sande, K. E.; Gevers, T.; and Smeulders, A. W. 2013. Selective search for object recognition. *International journal of computer vision*, 104(2): 154–171.

Wang, J.; and Specia, L. 2019. Phrase Localization Without Paired Training Examples. In *ICCV, Seoul, Korea (South)*, 4662–4671. IEEE.

Wang, L.; Li, Y.; Huang, J.; and Lazebnik, S. 2018. Learning two-branch neural networks for image-text matching tasks. *IEEE Transactions on Pattern Analysis and Machine Intelligence*, 41(2): 394–407.

Wang, L.; Li, Y.; and Lazebnik, S. 2016. Learning deep structure-preserving image-text embeddings. In *Proceedings of the IEEE conference on computer vision and pattern recognition*, 5005–5013.

Wang, M.; Azab, M.; Kojima, N.; Mihalcea, R.; and Deng, J. 2016. Structured matching for phrase localization. In *European Conference on Computer Vision*, 696–711. Springer.

Wu, F.; Xu, Z.; and Yang, Y. 2017. An end-to-end approach to natural language object retrieval via context-aware deep reinforcement learning. *arXiv preprint arXiv:1703.07579*.

Xiao, F.; Sigal, L.; and Jae Lee, Y. 2017. Weakly-supervised visual grounding of phrases with linguistic structures. In *Proceedings of the IEEE Conference on Computer Vision and Pattern Recognition*, 5945–5954.

Yang, Z.; Gong, B.; Wang, L.; Huang, W.; Yu, D.; and Luo, J. 2019. A fast and accurate one-stage approach to visual grounding. In *Proceedings of the IEEE/CVF International Conference on Computer Vision*, 4683–4693.

Yeh, R. A.; Xiong, J.; Hwu, W. W.; Do, M. N.; and Schwing, A. G. 2017. Interpretable and Globally Optimal Prediction for Textual Grounding using Image Concepts. In Guyon, I.; von Luxburg, U.; Bengio, S.; Wallach, H. M.; Fergus, R.; Vishwanathan, S. V. N.; and Garnett, R., eds., *Advances in Neural Information Processing Systems 30: Annual Conference on Neural Information Processing Systems 2017, December 4-9, 2017, Long Beach, CA, USA*, 1912–1922.

Young, P.; Lai, A.; Hodosh, M.; and Hockenmaier, J. 2014. From image descriptions to visual denotations: New similarity metrics for semantic inference over event descriptions. *TACL*, 2: 67–78.

Yu, L.; Poirson, P.; Yang, S.; Berg, A. C.; and Berg, T. L. 2016. Modeling context in referring expressions. In *European Conference on Computer Vision*, 69–85. Springer.

Yu, Z.; Yu, J.; Xiang, C.; Zhao, Z.; Tian, Q.; and Tao, D. 2018. Rethinking Diversified and Discriminative Proposal Generation for Visual Grounding. In Lang, J., ed., *Proceedings of the Twenty-Seventh International Joint Conference on Artificial Intelligence, IJCAI 2018, July 13-19, 2018, Stockholm, Sweden*, 1114–1120. ijcai.org.

Zhang, H.; Niu, Y.; and Chang, S.-F. 2018. Grounding referring expressions in images by variational context. In *Proceedings of the IEEE Conference on Computer Vision and Pattern Recognition*, 4158–4166.

Zhao, F.; Li, J.; Zhao, J.; and Feng, J. 2018. Weakly supervised phrase localization with multi-scale anchored transformer network. In *Proceedings of the IEEE Conference on Computer Vision and Pattern Recognition*, 5696–5705.

Zheng, Z.; Wang, P.; Liu, W.; Li, J.; Ye, R.; and Ren, D. 2020a. Distance-IoU loss: Faster and better learning for bounding box regression. In *Proceedings of the AAAI Conference on Artificial Intelligence*, volume 34, 12993–13000.

Zheng, Z.; Wang, P.; Ren, D.; Liu, W.; Ye, R.; Hu, Q.; and Zuo, W. 2020b. Enhancing geometric factors in model learning and inference for object detection and instance segmentation. *arXiv preprint arXiv:2005.03572*.

Zhou, B.; Tian, Y.; Sukhbaatar, S.; Szlam, A.; and Fergus, R. 2015. Simple baseline for visual question answering. *arXiv preprint arXiv:1512.02167*.

Zitnick, C. L.; and Dollár, P. 2014. Edge boxes: Locating object proposals from edges. In *European conference on computer vision*, 391–405. Springer.